Horwood NJ, Elliot J, Martin TJ, Gillespie MT. 1998. Osteotropic agents regulate the expression of osteoclast differentiation factor and osteoprotegerin in osteoclastic stromal cells. Endocrinology 39:4743–4746.

Houssami S, Findlay DM, O'Keeffe LM, Martin TJ, Sexton PM. 1994. Heterogeneity in ligand recognition of calcitonin receptors. Endocrine J 2:127–134.

Howe LR, Watanabe O, Leonard J, Brown AMC. 2003. Twist is up-regulated in response to Wnt1 and inhibits mouse mammary cell differentiation. Cancer Res 63: 1906–1913.

Hu E, Tontonoz P, Spiegelman BM. 1995. Transdifferentiation of myoblasts by the adipogenic transcription factors PPARγ and C/EBPα. Proc Natl Acad Sci USA 92:9856–9860.

Ingham PW. 1998. Transducing hedgehog: The story so far. EMBO J 17:3505–3511.

Javed A, Barnes GL, Jasanya BO, Stein JL, Gerstenfelf L, Lian JB, Stein GS. 2001. *runt* homology domain transcription factors (Runx, Cbfa, and AML) mediate repression of the bone sialoprotein promoter: Evidence for promoter context-dependent activity of Cbfa proteins. Mol Cell Biol 21:2891–2905.

Jiménez MJA, Balbín M, López JM, Alvarez J, Komori T, López-Otín C. 1999. Collagenase is a target of Cbfa1, a transcriptional factor of the *runt* gene family involved in bone formation. Mol Cell Biol 19:4431–4442.

Kato M, Patel MS, Levasseur R, Lobov I, Chang BH-J, Glass DA, Hartmann C, Li L, Hwang T-H, Brayton CF, Lang RA, Karsenty G, Chan L. 2002. Cbfa1-independent decrease in osteoblast proliferation, osteopenia, and persistent embryonic eye vascularization in mice deficient in Lrp5, a Wnt coreceptor. J Cell Biol 157:303–314.

Kern B, Shen J, Starbuck M, Karsenty G. 2001. Cbfa1 contributes to the osteoblast-specific expression of *type I collagen* genes. J Biol Chem 276:7101–7107.

Kim HJ, Rice DP, Kettunen PJ, Thesleff I. 1998. FGF-, BMP-, and Shh-mediated signalling pathways in the regulation of cranial suture morphogenesis and calvaria bone development. Devel 125:1241–1251.

Komori T, Yagi H, Sasaki K, Deguchi K, Shimizu Y, Bronson RT, Gao Y-H, Inada M, Sato M, Okamoto R, Kitamura Y, Yoshiki S, Kishimoto T. 1997. Targeted disruption of Cbfa1 results in a complete lack of bone formation owing to maturational arrest of osteoblasts. Cell 89:755–764.

Kondo H, Ohyama T, Ohya K, Kasugai S. 1997. Temporal changes of mRNA expression of matrix proteins and parathyroid hormone and parathyroid hormone-related protein (PTH/PTHrP) receptor in bone development. J Bone Miner Res 12:2089–2097.

Krishnan V, Moore TL, Ma YL, Helvering LM, Frolik CA, Valasek KM, Ducy P, Geiser AG. 2003. Parathyroid hormone bone anabolic action requires cbfa1/runx2-dependent signaling. Mol Endocrinol 17:423–435.

Kuri-Haruch W, Green H. 1978. Adipose conversion of 3T3 cells depends on a serum factor. Proc Natl Acad Sci USA 75:6107–6109.

Lecka-Czernik B, Gubrij I, Moerman EJ, Kajkenova O, Lipschit DA. 1999. Inhibition of Osf2/Cbfa1 expression and terminal osteoblast differentiation by PPARγ2. J Cell Biochem 74:357–371.

Lecka-Czernik B, Moerman EJ, Grant DF, Lehmann JM, Manolagas SC, Jilka RL. 2002. Divergent effects of selective peroxisome proliferator-activated receptor-γ2 ligands on adipocyte versus osteoblast differentiation. Endocinol 143:2376–2384.

Lee M-S, Lowe GN, Strong DD, Wergedeal JE, Glackin CA. 1999. Twist, a basic helix-loop-helix transcription factor, can regulate the human osteogenic lineage. J Cell Biochem 75:566–577.

Nakashima K, Zhou X, Kunkel G, Zhang Z, Deng JM, Behringer RR, de Crombrugghe B. 2002. The Novel Zinc finger-containing transcription factor osterix is required for osteoblast differentiation and bone formation. Cell 108:17–29.

Nuttal ME, Patton AJ, Olivera DL, Nadeau DP, Gowen M. 1998. Human trabecular bone cells are able to express both osteoblastic and adipocytic phenotype: Implications for osteogenic disorders. J Bone Miner Res 13: 371–382.

Oreffo ROC, Virdi AS, Triffit JT. 1997. Modulation of osteogenesis and adipogenesis by human serum in human bone marrow cultures. Eur J Cell Biol 74:251–261.

Oshima A, Tanabe H, Yan T, Lowe GN, Glackin CA, Kudo A. 2002. A novel mechanism for the regulation of osteoblast differentiation: Transcription of periostin, a member of the fasciclin 1 family, is regulated by the bHLH transcription factor Twist. J Cell Biochem 86:792–804.

Otto F, Thornell AP, Crompton Denzel A, Gilmour KC, Rosewell IR, Stamp GWH, Beddongton RSP, Mumdlos S, Olsen BR, Selby PB, Owen MJ. 1997. *Cbfa1*, a candidate gene for cleidocranial dysplasia syndrome, is essential for osteoblast differentiation and bone development. Cell 89:765–771.

Owen ME. 1985. Lineage of osteogenic cells and their relationship to the stromal system. In: Peck WA, editor. Bone and mineral research, Vol 3. Amsterdam, New York, Oxford: Elsevier. pp 1–25.

Park SR, Oreffo ROC, Triffit JT. 1999. Interconversion potential of cloned human marrow adipocytes in vitro. Bone 24:549–554.

Partridge NC, Alcorn D, Michelangeli VP, Kemp BE, Ryan GB, Martin TJ. 1981. Functional properties of hormonally responsive cultured normal and malignant rat osteoblastic cells. Endocrinol 108:213–219.

Ross SE, Hemati N, Longo KA, Bennet CN, Lucas PC, Erickson RL, MacDougald OA. 2000. Inhibition of adipogenesis by Wnt signalling. Science 289:950–953.

Sato M, Morii E, Komori T, Kawahata H, Sugimoto M, Terai K, Shimizu H, Yasui T, Ogihara H, Yasui N, Ochi T, Kitamura Y, Ito Y, Nomura S. 1998. Transcriptional regulation of osteopontin gene in vivo by PEBP2-alpha CBFA1 and ETS1 in the skeletal tissues. Oncogene 17:1517–1525.

Selvanmurugan N, Pulumati MR, Tyson DR, Partridge NC. 2000. Parathyroid hormone regulation of the rat collagenase-3 promoter by protein kinase A-dependent transactivation of core binding factor α1. J Biol Chem 275:5037–5042.

Shui C, Spelberg TC, Riggs BL, Khosla S. 2003. Changes in Runx2/Cbfa1 expression and activity during osteoblastic differentiation of human bone marrow stromal cells. J Bone Miner Res 18:213–221.

Spinella-Jaegl S, Rawadi G, Kawai S, Gallea S, Faucheu C, Mollat P, Coutrois B, Bergaud B, Ramez V, Blanchet AM, Adelmant G, Baron R, Roman-Roman S. 2001. Sonic

hedgehog increases the commitment of pluripotent mesenchymal cells into the osteoblastic lineage and abolishes adipocytic differentiation. J Cell Sci 114:2085–2091.

St-Jacques B, Hammerschmidt M, McMahon AP. 1999. Indian hedgehog signalling regulates proliferation of chondrocytes and is essential for bone formation. Genes Dev 13:2072–2086.

Stanford CM, Jacobson PA, Eanes ED, Lembke LA, Midura RJ. 1995. Rapidly forming apatitic mineral in an osteoblastic cell line (UMR106-01BSP). J Biol Chem 270:9420–9428.

Thirunavukkarasu K, Halladay DL, Miles RR, Yang XH, Galvin RJS, Chandrasekhar S, Martin TJ, Onyia JE. 2000. The osteoblast-specific transcription factor Cbfa1 contributes to the expression of osteoprotegerin, a potent inhibitor of osteoclast differentiation and function. J Biol Chem 275:25163–25172.

Umezawa A, Maruyama T, Segawa K, Shadduck R, Waheed A, Hata J-I. 1992. Multipotent marrow stromal cell line is able to induce hematopoiesis in vivo. J Cell Physiol 151:197–205.

Wennberg C, Hessle L, Lunberg P, Mauro S, Narisawa C, Lerner UF, Millan JL. 2000. Functional characterization of osteoblasts and osteoclasts from alkaline phosphatase knockout mice. J Bone Miner Res 15:1879–1888.

Xiao G, Wang D, Douglas M, Karsenty G, Franceshi RT. 1998. Role of the α2-integrin in osteoblast-specific gene expression and activation of the Osf2 transcription factor. J Biol Chem 273:32988–32994.

Yousfi M, Lasmoles F, Kern B, Marie PJ. 2002. Twist inactivation reduces CBFA1/RUNX2 expression and DNA binding to the osteocalin promoter in osteoblasts. Biochem Biophys Res Commun 297:641–644.

Yuasa T, Kataoka H, Kinto N, Iwamoto M, Enomoto-Iwamoto M, Iemura S-I, Ueno N, Shibata Y, Kurosawa H, Yamaguchi A. 2002. Sonic hedgehog is involved in osteoblast differentiation by cooperating with BMP-2. J Cell Physiol 193:225–232.

ACADEMIC PRESS

Available online at www.sciencedirect.com

SCIENCE DIRECT®

Experimental Cell Research 290 (2003) 370–380

Experimental Cell Research

www.elsevier.com/locate/yexcr

Osteogenic differentiation of the mesenchymal progenitor cells, Kusa is suppressed by Notch signaling

Kentaro Shindo,[a,*] Nobuyuki Kawashima,[a,1] Kei Sakamoto,[b,1] Akira Yamaguchi,[c] Akihiro Umezawa,[d] Minoru Takagi,[b] Ken-ichi Katsube,[b,*] and Hideaki Suda[a]

[a] *Pulp Biology and Endodontics, Graduate School of Tokyo Medical and Dental University, 1-5-45, Yushima, Bunkyo-ku, Tokyo 113-8549, Japan*
[b] *Molecular Pathology, Graduate School of Tokyo Medical and Dental University, 1-5-45, Yushima, Bunkyo-ku, Tokyo 113-8549, Japan*
[c] *Oral Pathology and Bone Metabolism, Biomedical Graduate School of Nagasaki University, 1-7-1, Sakamoto, Nagasaki 852-8588, Japan*
[d] *Department of Reproductive Biology and Pathology, National Research Institute for Child Health and Development, 3-35-31, Taishido, Setagaya-ku, Tokyo 154-8567, Japan*

Received 4 February 2003, revised version received 10 June 2003

Abstract

Notch receptor plays a crucial role in proliferation and differentiation of many cell types. To elucidate the function of Notch signaling in osteogenesis, we transfected the constitutively active *Notch1* (*Notch* intracellular domain, *NICD*) into two different osteoblastic mesenchymal cell lines, KusaA and KusaO, and examined the changes of their osteogenic potentials. In *NICD* stable transformants (KusaA^{NICD} and KusaO^{NICD}), osteogenic properties including alkaline phosphatase activity, expression of osteocalcin and type I collagen, and in vitro calcification were suppressed. Transient transfection of *NICD* attenuated the promoter activities of *Cbfa1* and *Ose2* element. KusaA was capable of forming trabecular bone-like tissues when injected into mouse abdomen, but this in vivo bone forming activity was significantly suppressed in KusaA^{NICD}. Osteoclasts were induced in the KusaA-derived bone-like tissues, but lacked in the KusaA^{NICD}-derived tissues. These results suggest that Notch signaling suppresses the osteoblastic differentiation of mesenchymal progenitor cells.
© 2003 Elsevier Inc. All rights reserved.

Keywords: Osteogenesis; Mineralization; Mesenchymal progenitor cells; Kusa; Notch; RANKL

Introduction

The bone marrow stromal cells have been shown to have a potential to differentiate into a variety of mesenchymal cells, such as adipocytes, chondrocytes, and myocytes. The properties as multipotent progenitor cells make them an attractive target for use in therapeutic and bioengineering applications, and the regulation of their commitment to specific cell types is a field of primary interest [1,2].

Osteogenic lineage is one differentiation pathway of bone marrow progenitor cells. Many factors are involved in differentiation of osteoblasts and their importance in regulating proliferation and differentiation has been well documented, but the molecular processes controlling their lineage commitment and self-renewal are yet to be elucidated [3,4].

Notch signaling is an intercellular communication system that is conserved among the multicellular organisms, which is believed to be crucial for fate determination of stem cells and progenitor cells [5,6]. Notch is a single-pass transmembrane receptor with an extracellular domain that recognizes the DSL (Delta/Serrate/Lag2) type ligands on the surface of adjacent cells [7]. Notch signal is transduced through several different pathways. As one of them, association with the ligands induces several sequential proteolytic cleavages, which results in the release of the intracellular domain from the plasma membrane [8]. The internalized intracellular domain of Notch translocates to the nucleus, where it interacts with a DNA binding protein,

* Corresponding authors. Fax: +81-3-5803-5494 and Fax: +81-3-5803-0188.
E-mail addresses: k.shindo.endo@tmd.ac.jp (K. Shindo), katsube.mpa@tmd.ac.jp (K. Katsube).
[1] These authors contributed equally to this work.

0014-4827/$ – see front matter © 2003 Elsevier Inc. All rights reserved.
doi:10.1016/S0014-4827(03)00349-5

CBF1 to control the expression of downstream genes, including *HES* transcription factors [9,10]. In various situations, the effect of Notch signaling seems to regulate a phenomenon called "lateral specification." In lateral specification, the cells committed to the primary differentiation fate express the DSL ligand and stimulate Notch signaling pathway in juxtaposed cells, which prevents their differentiation and directs them to remain in an uncommitted state [11,12]. The concept that Notch signaling inhibits differentiation has been postulated by many studies that utilize the constitutively active form of *Notch* [13,14]. Overexpression of constitutively active *Notch* suppresses the differentiation of neurogenic or hematopoietic stem cell lines, suggesting that Notch signaling is essential for control of cell differentiation [15,16].

An accumulating body of evidence indicates that Notch signaling also mediates the generation of mesenchymal tissues, such as in myogenesis and angiogenesis [17–19]. The expression of *Notch* and its related genes is also observed in the cells that are recruited to cartilage and bone formation. *Notch2* and *Delta1* are co-expressed in chondrocytes [20]. *Notch2* is expressed by periosteal cells, osteoblasts, and osteocytes in the region of active bone formation [21]. In a human osteosarcoma cell line, SAOS-2, the expression of *Notch1, Notch2* and *Notch4* is differentially regulated upon osteogenic stimulation [22]. These observations raise the possibility that Notch signaling may also regulate the growth and differentiation of osteogenic cells, playing an important role in bone formation.

Here, we present evidence that Notch signaling has a suppressive role in osteoblastic differentiation, using mesenchymal progenitor cell lines, KusaA and KusaO [23–25].

Materials and methods

Cell culture and DNA transfection

KusaA was the original cell line established and described as Kusa [23]. Later, KusaO was subcloned as a non-osteogenic subline of Kusa during passage. KusaA and KusaO were named after this process, but the difference of their property was not well studied. KusaA is at a more advanced stage of osteoblastic differentiation compared to KusaO. Cells were cultured in α-MEM containing 10% fetal bovine serum. Constitutively active form of mouse *Notch1* (*Notch intra cellular domain, NICD*) was a gift from J. Nye. Dominant negative form of chicken *Delta* (*dnDl*) has been previously described [26]. Each DNA was recombined in a mammalian expression vector, pcDNA3 (Invitrogen). Transfection was performed using LipofectAmine 2000 (Invitrogen) according to the manufacturer's instructions. Cells stably expressing *NICD* were selected with 500 μg/ml Geneticin (Invitrogen) and expanded after single colony isolation.

Reverse transcription-polymerase chain reaction (RT-PCR)

RNA was extracted using TRIzol (Invitrogen). One microgram of total RNA was reverse-transcribed with Superscript II (Invitrogen) using oligo-dT primers. Using this cDNA as a template, polymerase chain reaction (PCR) was performed. The sequences of the PCR primers for mouse *Notch1* were: upper 5′-CTTGCAGTAG-CAAGGAAGCTAAGG-3′ and lower 5′-ACTTAAAT-GCCTCTGGAATGTCG-3′. The PCR parameters for *Notch1* were: 25 cycles at 94°C for 30 seconds, 55°C for 30 seconds, and 72°C for 60 seconds. The sequences of the PCR primers for mouse *RANKL* were: upper 5′-GGTCGGGCAATTCTGAATT-3′ and lower 5′-GG-GAATTACAAAGTGCACCAG-3′. The PCR parameters for *RANKL* were: 35 cycles at 94°C for 30 seconds, 55°C for 30 seconds, and 72°C for 60 seconds. The amplified products were electrophoresed in a 1.5% agarose gel and stained with ethidium bromide [27].

Western blot analysis

Cells grown in 35 mm^2 culture vessels were washed twice with phosphate buffered saline and lysed with TNTC buffer (100 mM Tris-Cl, pH 7.6; 150 mM NaCl; 1 mM $CaCl_2$; 1% Triton X-100 containing protease inhibitors (Complete; Roche)). The lysate was mixed with 2× loading buffer containing 40 mM DTT and boiled for two minutes. The proteins were electrophoresed in an 8% polyacrylamide gel containing SDS and transferred to a nitrocellulose membrane (Hybond-C Extra; Amersham Pharmacia Biotech). Protein detection was performed using anti-Notch1 cytoplasmic domain antibody (Upstate Biotechnology).

Measurement of alkaline phosphatase (ALP) activity and calcium deposition

ALP activity was measured using the ALP measurement kit (ALP-K Test; Wako Chemicals). The amount of calcium deposits on culture dishes was measured using the calcium measurement kit (Ca-E Test; Wako Chemicals). Protein concentrations were measured for normalization using the DC Protein Assay Kit (Bio-Rad).

Northern blot analysis

Ten micrograms of total RNA from each cell line were electrophoresed in a 1.2% agarose formaldehyde gel. The RNA was transferred to a charged nylon membrane (Hybond-N+; Amersham Pharmacia Biotech). cDNA of *Collagen type I* (*Col I*) and *Osteocalcin* (*OC*) were labeled with [α-^{32}P]dCTP using the Ready-To-Go DNA Labeling Beads (Amersham Pharmacia Biotech). Hybridization was performed overnight at 42°C and the membrane was thoroughly washed with 0.1× salt sodium citrate (15 mM NaCl and 1.5 mM trisodium citrate). Radioactive signals were

detected using a digital image analyzer (Bas2500; Fuji Photo Film). Densitometrical analysis was carried out using Photoshop 5.5 (Adobe). The mouse *OC* cDNA was provided by J.M. Wozney and the α2 chain of rat type I collagen cDNA was provided by C. Genoverse.

Luciferase activity assay

Fifty percent confluent cells were transiently transfected with *NICD*. The cells were harvested 48 h after the transfection and luciferase activity was measured, using the Dual Luciferase Reporter Assay System (Promega). To see the effect of Notch signal suppression, we used the *dnDl* (dominant negative *Delta*) construct, which can inhibit Notch signal transduction to *Hes1* pathway in a cell-autonomous manner [26]. All experiments were performed in triplicate and the *firefly* luciferase activity was normalized to the co-transfected *Renilla* luciferase activity (pRL-EF, a gift from Y. Mochida). Statistical data analysis was carried out using Excel 2000 (Microsoft). The *Ose2* elements and the *Cbfa1* promoter were provided by Sumitomo Pharmaceuticals Research Center [28].

In vitro mineralization assay

To promote mineralization, 0.2 mM of L-ascorbic acid-2-phosphate (AA) and 10 mM of β-glycerophosphate (βGP) were added to the culture medium after the cells reached confluence. Cells were left confluent for several days with or without AA and βGP to allow mineralization. Calcified nodules were stained with Alizarin Red S after methanol fixation. The amount of calcification was evaluated by digitally measuring the stained areas using a computer software (Scion Image; Scion Corporation).

In vivo osteogenesis assay

Cells were grown to confluence and trypsinized to collect 1×10^8 cells/ml in 100 μl of medium. The cells were subcutaneously injected into the abdomen of C3H/He mice with an 18G syringe. Thirty days after inoculation, the animals were sacrificed and soft X-ray photos were taken to detect calcification. The tissues originating from the injected cells were dissected and processed for histological analyses. Non-decalcified 4 μm thick sections were stained with hematoxylin and eosin, von Kossa's, ALP and TRAP (tartarate resistant acid phophatase) staining methods.

Results

Constitutively active Notch suppresses the expression of osteogenic marker genes in Kusa

In order to evaluate the stem cell property of Kusa, we established the stable transformants of the constitutively active form of *Notch1* (*NICD*) driven by the cytomegalovirus promoter in both KusaA and KusaO cell lines (KusaA^{NICD} and KusaO^{NICD}). RT-PCR using the primers set within the *NICD* region revealed endogenous expression of *Notch1* in the original KusaA and KusaO, along with robust PCR amplification due to *NICD* in the KusaA^{NICD} and KusaO^{NICD} (Fig. 1A). Western blot analysis showed an identical level of NICD protein in the KusaA^{NICD} and KusaO^{NICD}, but the endogenous Notch1 protein was far below the threshold of detection (Fig. 1A). In the *NICD* transformants, *HES1* promoter was activated more than 100 fold (Fig. 1B) of its basal level. The *NICD* transformants were morphologically indiscriminate from the original cells. Each cell line proliferated at the same rate, with a doubling time of about 20 h (data not shown). To evaluate the osteogenic potential, ALP activity and the expression of *Coll* and *OC* were examined under normal culture condition and mineralization-promoting condition by addition of ascorbic acid (AA) and β-glycerophosphate (βGP) to the medium. We found that *NICD* suppressed ALP activity and the expression of *OC* in KusaA, (Figs. 2A, 2C, and 2E). The basal level of ALP activity in KusaO with or without *NICD* is far less than that in KusaA (Fig. 2B). *Coll* expression in KusaO increased after confluence, especially under mineralization-inducing condition, but this upregulation of *Col I* was suppressed by

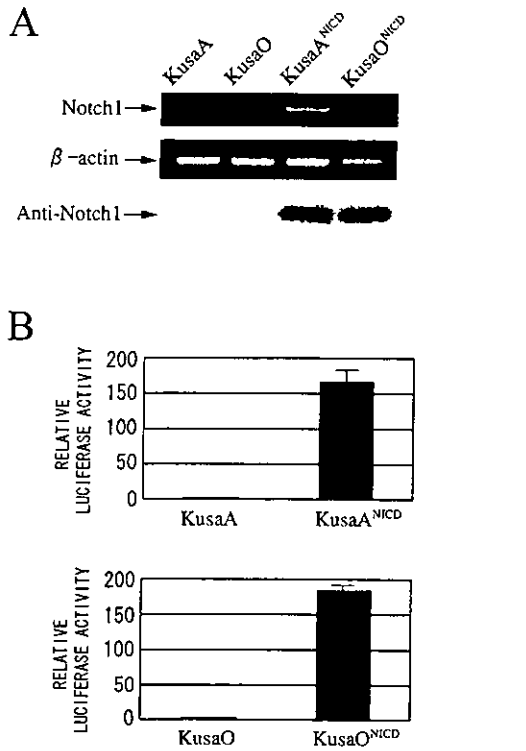

Fig. 1. Establishment of *NICD* stable transformants. (A) RT-PCR demonstrated the endogenous *Notch1* expression, and intense amplifications due to the integrated *NICD* in KusaA^{NICD} and KusaO^{NICD} (top row). Western blot analysis revealed the expression of 150 KDa NICD protein in KusaA^{NICD} and KusaO^{NICD}. The endogenous expression of Notch protein was below the threshold of detection (bottom row). (B) *HES1* promoter activity was significantly elevated in KusaA^{NICD} and KusaO^{NICD}.

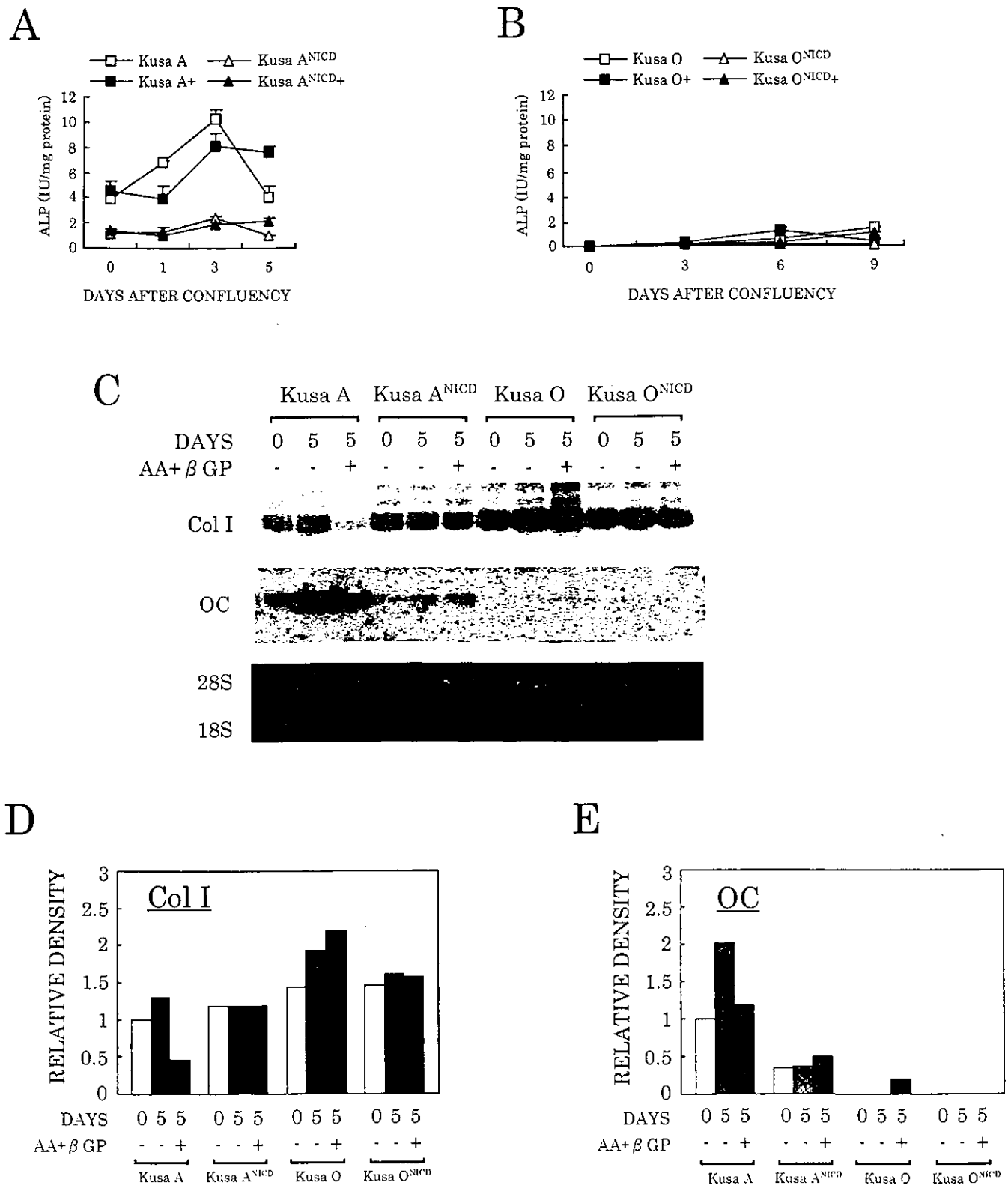

Fig. 2. Suppression of osteogenic properties in KusaA^{NICD} and KusaO^{NICD}. (A) Assay for alkaline phosphatase (ALP) activity. KusaA exhibited constantly high ALP activity, which was suppressed in KusaA^{NICD}. Cells cultured in the medium containing ascorbic acid and β-glycerophosphate are marked with a '+'. (B) ALP activity of KusaO was low with or without NICD. (C) Northern blot analysis of *Col I* and *OC*. (D, E) Densitometrical analysis of (C) shows the expression of *OC* in KusaA and *Col I* in KusaO was suppressed by NICD.

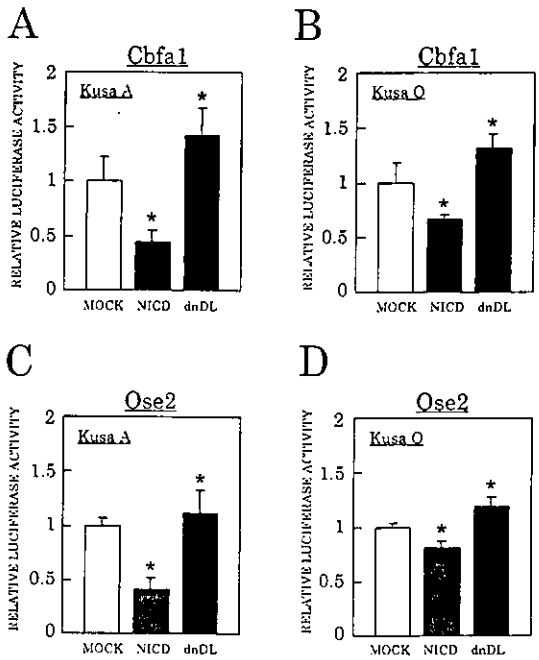

Fig. 3. Promoter activity assay for *Cbfa1* and *Ose2* elements in KusaA and KusaO with *NICD* transient transfection. (A–D) Promoter activities of *Cbfa1* and *Ose2* elements were reduced by *NICD* in both KusaA and KusaO. On the contrary, KusaA and KusaO transfected with an antagonist of Notch signaling, *dnDL* (*dominant negative Delta*), exhibited elevated promoter activities of *Cbfa1* and *Ose2*. Each bar represents the mean ± 1 SD.

NICD (Figs. 2C–D). KusaO slightly upregulated *OC* under the mineralization-inducing condition, which was not observed in KusaO^{NICD} (Figs. 2C and E).

Promoter activity of Cbfa1 and Ose2 was attenuated by NICD

Gene expression of *Col I* and *OC*, is partially under the control of *Ose2* elements in their promoters [29,30]. *Ose2* is a consensus binding site of Cbfa1 [31], which is a key transcription factor to regulate osteoblast differentiation and bone formation.

We examined the effect of Notch signal activation on the promoter activities of *Cbfa1* and *Ose2* in Kusa. The activity of *Cbfa1* promoter was attenuated by *NICD* both in KusaA and KusaO (Figs. 3A–B), indicating that the Notch signaling has an inhibitory effect on the transcription of *Cbfa1*. We also observed a modest increase of *Cbfa1* promoter activity by dnDl, implying that the expression of *Cbfa1* is being suppressed by endogenous Notch signaling in Kusa cells. Promoter activity of *Ose2* was also attenuated by *NICD* (Figs. 3C–D), which is consistent with the downregulation of *OC*, and the downregulation of *Col1* in KusaO, as shown in the northern analysis.

Calcium deposition and calcified nodule formation in vitro were reduced by NICD

In the presence of AA and βGP, calcium deposition gradually increased after confluence both in KusaA and KusaO, where KusaA exhibited a more rapid rise (Figs. 4A–B). KusaA^{NICD} and KusaO^{NICD} also showed a gradual increase in calcium deposition, but it was much slower and the amount was significantly reduced. Calcified nodules were formed only in the presence of AA and βGP. The amount of calcified nodules formed by KusaA^{NICD} was reduced to less than half of that formed by KusaA (Figs. 4C and E). KusaO also formed calcified nodules, although slower than KusaA. KusaO^{NICD} cells failed to form a calcified nodule (Figs. 4D–E).

In vivo bone formation of KusaA was suppressed by NICD

To assess the effect of Notch signaling to the osteogenic potential of Kusa in vivo, we subcutaneously injected the cultured cells into mouse abdomen and examined them after 30 days. In most cases of KusaA (9/10), the injected cells proliferated and formed a nodular mass about 7 mm in diameter that was readily identified and separated from the surrounding tissues. These masses contained calcified tissues that were observed as radiopaque foci (Figs. 5A–B). In KusaA^{NICD}, small patchy radiopaque structures were observed in some cases (4/10) (Figs. 5A and C) along with the other cases (6/10) that showed no radiopacity. In KusaO, no radiopaque image was observed with or without NICD (10/10, 10/10) (Fig. 5A).

In histology, KusaA showed a well-formed bone like structure (Fig. 6A), but KusaA^{NICD} showed small masses of calcification in fibrous tissues (Fig. 6B). In a magnified view, KusaA showed a fine structure of trabecular bone tissues (Fig. 6C), but KusaA^{NICD} showed amorphous calcified masses (Fig. 6D). The trabecular bone-like structures of KusaA were surrounded by ALP-positive spindle cells (Fig. 6E) and multinucleated TRAP-positive cells were observed adjacent to the trabecular (Fig. 6G). The other cell types such as nerve cells, capillary cells and myocytes, were not observed. No inflammatory cells were observed in the mass. KusaA^{NICD} also formed a mass that was easily separated from the surrounding tissues, but the formation of trabecular bone-like structures was not observed, except only a few small foci of amorphous calcification (Fig. 6D) that were surrounded by a few ALP-positive cells (Fig. 6F). TRAP-positive cells were not observed in the KusaA^{NICD}-derived tissues (Fig. 6H). The expression of *RANKL*, a factor of osteoclastogenesis secreted by osteoblastic cells, was detected by RT-PCR in KusaA, but was not observed in KusaA^{NICD} (Fig. 7).

Discussion

The process of osteogenesis can be divided into several steps, consisting of cell proliferation, extracellular matrix maturation and mineralization [32,33]. Initially, osteoblasts actively proliferate and produce extracellular matrix pro-

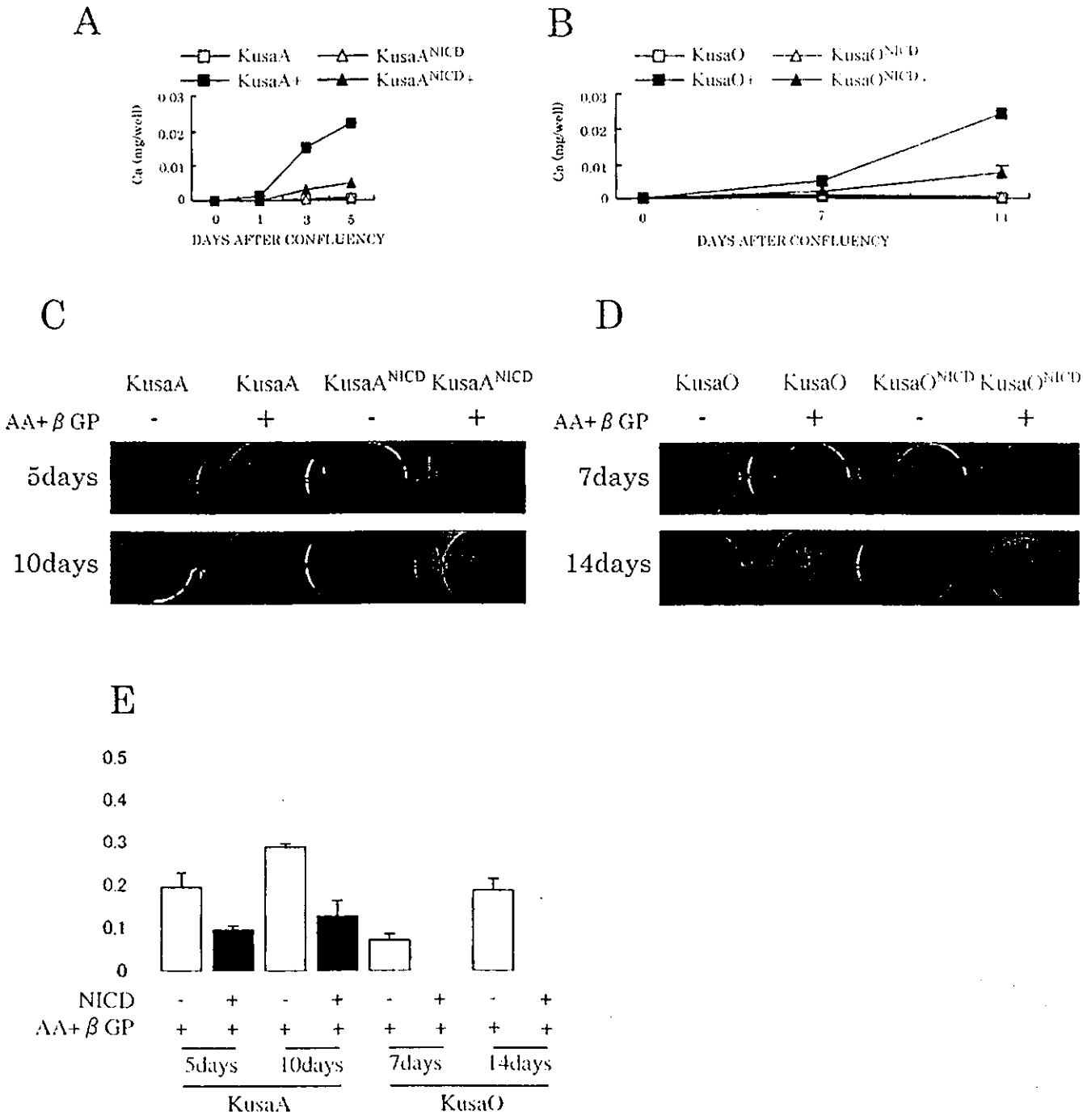

Fig. 4. In vitro calcification assay. (A, B) Quantification of calcium deposition on culture dish. "+" represents the addition of ascorbic acid and β glycerophosphate to the culture medium (filled squares and triangles in the graph). (C, D) Calcification on culture dishes stained with Alizarin Red S. (E) Graphical representation of (C) and (D).

teins, such as fibronectin or Col I. Once the matrix has matured, osteoblasts cease to divide but become to actively engage in the synergetic synthesis of matrix proteins. This step is accompanied with enhanced expression of alkaline phosphatase (ALP) that is assumed to metabolize phosphate ions into insoluble phosphate salts, such as calcium phosphate [34,35]. Later, upregulation of *OC* and osteopontin, which are the major non-collagenous bone matrix proteins, contributes to the refinement of extracellular matrices for calcification.

We demonstrated that Notch signaling downregulated the early osteoblastic marker *Col I* in KusaO and the late osteoblastic marker *OC* in KusaA, implying that Notch signaling exerts an inhibitory effect at various stages of osteoblastic differentiation. In hematopoietic progenitor cells, *NICD* inhibits granulocyte differentiation and permits

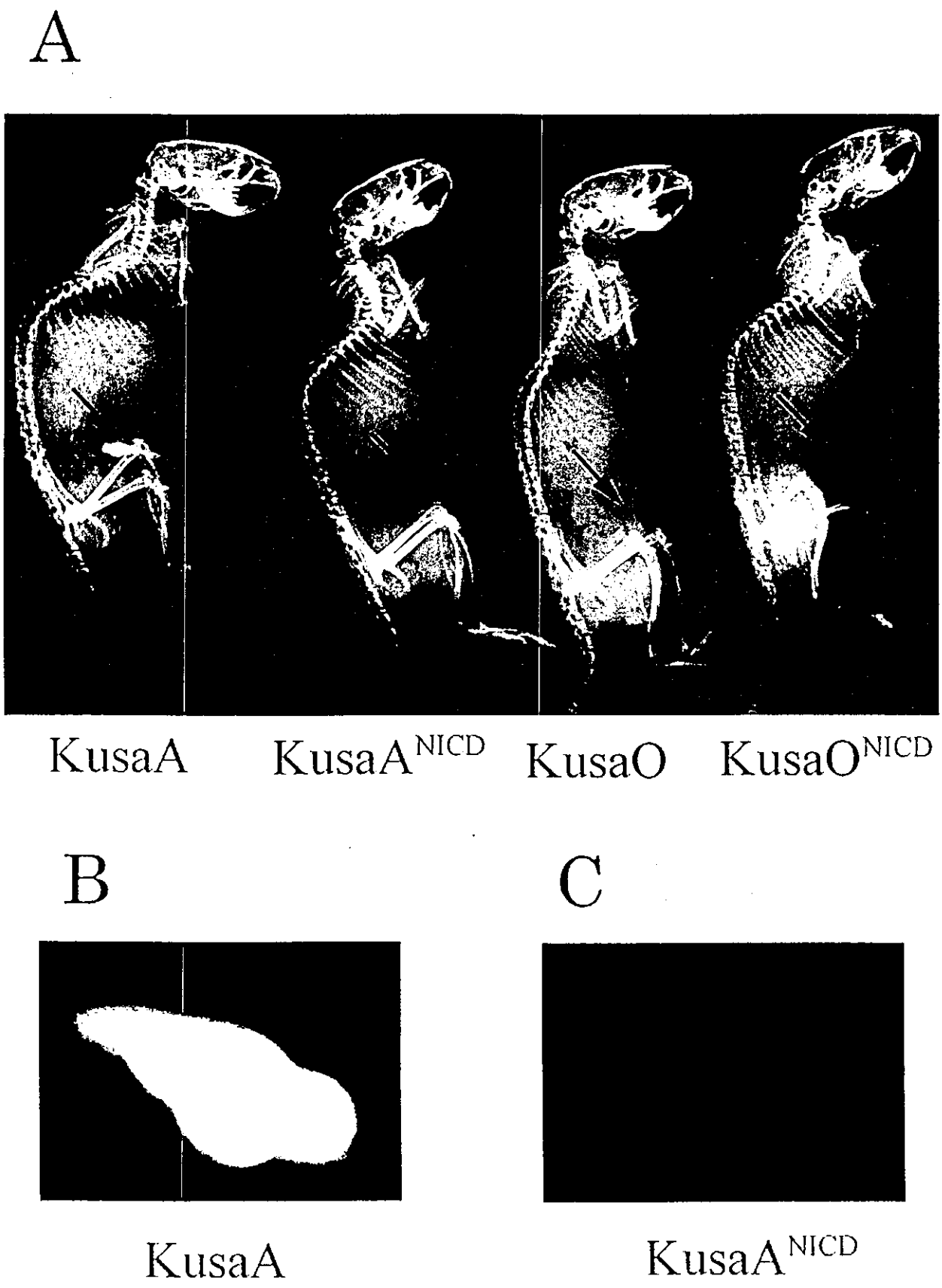

Fig. 5. Radiography of in vivo osteogenesis of Kusa cells. (A, B, C) Soft X ray photographs revealed that KusaA formed a distinct radiopaque mass in vivo, while KusaA^{NICD} formed a mass of the smaller size that is mainly radiolucent. KusaO and KusaO^{NICD} did not form a radio opaque mass.

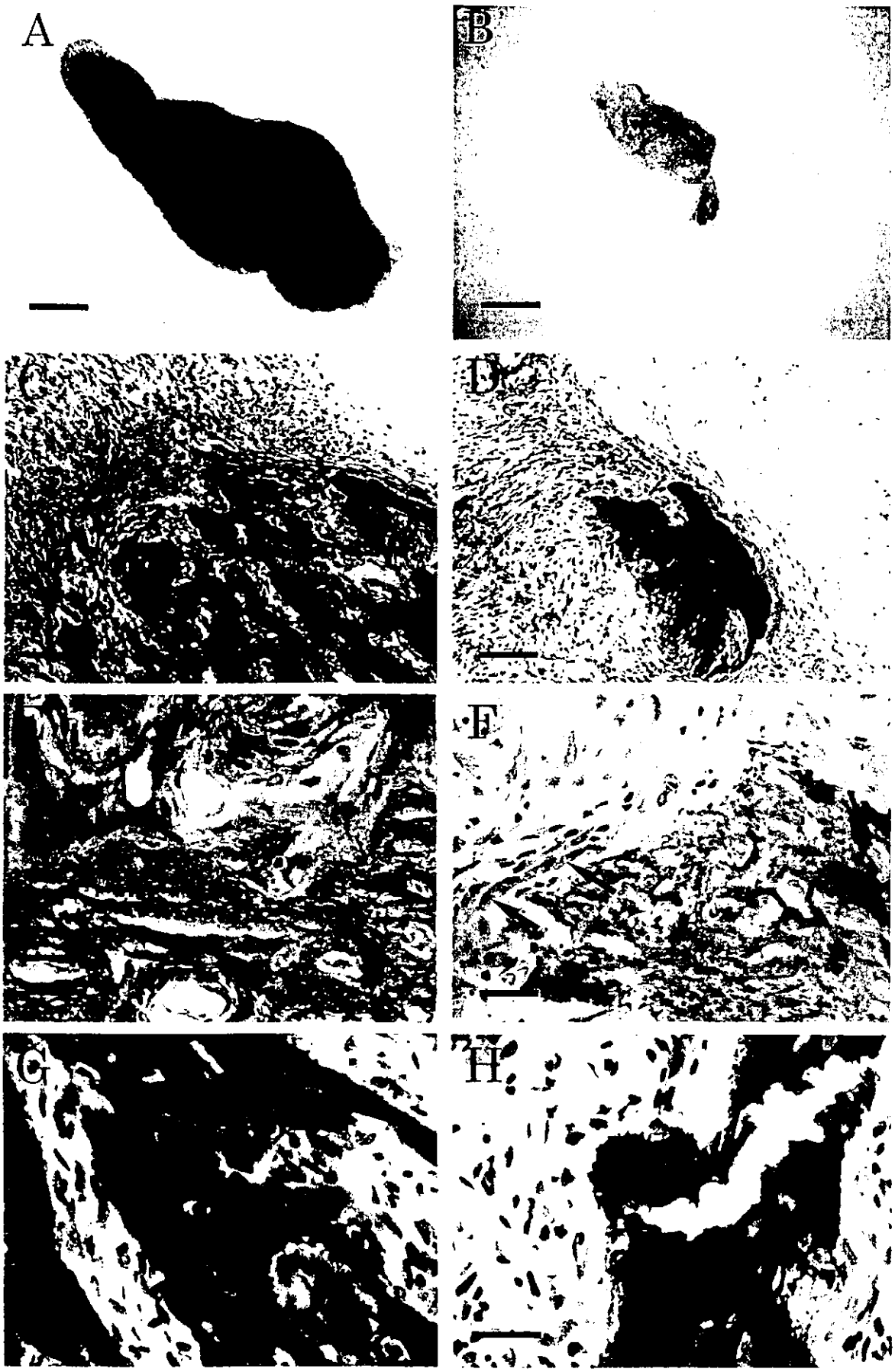
A
B
C
D
E
G
H

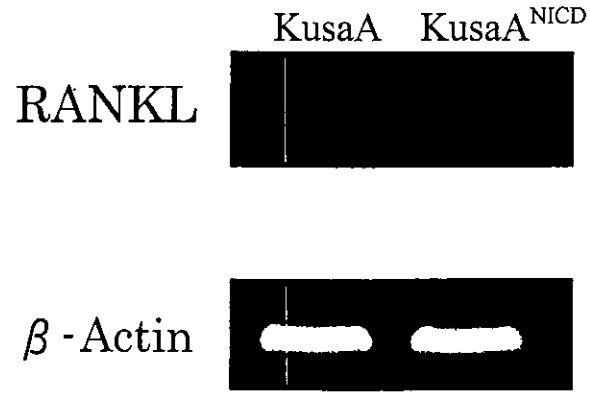

Fig. 7. *RANKL* expression in KusaA and KusaA^{NICD}. RT-PCR revealed expression of *RANKL* in KusaA, but not in KusaA^{NICD}.

the expansion of undifferentiated cells [14]. In neurogenesis, both neuronal and glial differentiation in vitro are enhanced by the attenuation of Notch signaling and suppressed by *NICD* [36,37]. These studies indicate that the activation of Notch signaling usually promotes the self-renewal of progenitor cells and inhibits their differentiation. In the present study, Notch signaling had little effect on Kusa cell proliferation, and the regulation of cell differentiation appeared to be its major role. The pattern of in vitro nodule formation was altered by *NICD*. The nodules of KusaA and KusaO had discrete margins, but those of KusaA^{NICD} and KusaO^{NICD} had ambiguous margins. This difference may reflect an activation of NICD, which inhibits "Salt and Pepper" pattern (an expression of lateral inhibition or lateral specification) formation.

Cbfa1 is a Runt-family transcription factor that acts as a key gene for osteoblast differentiation. Cbfa1 is a positive regulator of osteoblast-specific gene expression, where it can upregulate both *Col I* [29] and *OC* by binding to the *OSE2* elements in their promoters [31,38]. Although the relationship between Notch signaling and Cbfa1 has not been well studied, Hes1 has been reported to physically interact with Cbfa1 and cause a Cbfa1-dependent transactivation of the downstream genes [30,38]. These findings imply a possible connection between the Notch signaling pathway and Cbfa1-mediated osteogenesis. Transient expression of *NICD* in an osteoblastic cell line, MC3T3-E1 using an adenoviral vector reportedly led to upregulation of *Cbfa1* and even to increased calcified nodule formation in long-term cultures, but this effect appeared to be due to an accumulation in matrix proteins followed by delayed nodule formation [39]. Contrary to this report, we found that *NICD* modestly suppressed the promoter activity of *Cbfa1* and *Ose2*, and general suppression of osteogenesis in Kusa cells. Since the suppression of *Ose2* activity by *NICD* was also observed in COS7 cells (our unpublished data) that do not express *Cbfa1* [40], the negative effect of Notch signaling on osteogenesis may also occur in a Cbfa1-independent manner. In myogenesis, it has been postulated that the Notch signaling regulates the myoblasts differentiation by two different transduction pathways [41]. CBF1-dependent pathway appears to control the myogenic differentiation of C2C12, whereas Notch signaling in the absence of CBF1 blocks its myogenic and also osteogenic differentiation, indicating the presence of CBF1-independent pathway that leads to a pan-block of cell differentiation. The effect of CBF1 and its relationship with *Cbfa1* promoter in Kusa is now in the focus of interest.

By our preliminary experiments, slight expression of *Notch* and *Hes1* was detected, which indicates the endogenous activation of Notch signaling. Strong osteogenic properties of Kusa may be attributed to the suppression of endogenous Notch signaling by some mechanism. Interestingly, TRAP-positive osteoclasts were not observed in the bone-like tissues generated by KusaA^{NICD}. Osteoclast differentiation is in part triggered by factors from osteoblasts. RANKL, an osteoclast-differentiating factor, which belongs to the tumor necrosis factor ligand gene family, has been found in cells of osteoblastic lineage [42]. Osteoclast progenitors express RANK, a receptor of RANKL and differentiate into osteoclasts through cell-cell interactions with osteoblasts [43,44]. The *RANKL* expression was suppressed in KusaA^{NICD}, implying that this suppression resulted in the loss of osteoclast induction in vivo. Two putative Cbfa1 binding sites exist in the promoter region of *RANKL*, and upregulation of *RANKL* was observed following treatment with vitamin D3, which was accompanied with *Cbfa1* upregulation [45].

Downregulation of *RANKL* in KusaA^{NICD} may be due to the low activation of *Cbfa1*. However, a conflicting result has also been reported that *Cbfa1* overexpression had no effect on upregulation of *RANKL* [46]. The association of Notch signaling with Cbfa1 pathway remains to be elucidated.

In conclusion, we demonstrated that the constitutively active form of Notch1 suppresses the osteoblastic differentiation and osteoclastogenesis of Kusa cells, suggesting that the Notch signaling negatively regulates the bone formation and its refinement. Our findings reinforce the possibility of a new therapeutic strategy for the treatment of bone diseases

Fig. 6. In vivo osteogenesis of KusaA and KusaA^{NICD}. Histology of KusaA-derived tissues (A) and KusaA^{NICD}-derived tissues (B). (C) Higher magnification of (A) shows fibrous tissues with trabecular bone-like tissues. (D) Higher magnification of (B) shows fibrous tissues and a small mass of calcification without a trabecular structure. (E) ALP staining showed that bone-like tissues derived from KusaA were surrounded by numerous spindle shaped cells positive for ALP (colored in purple), implying the presence of osteoblasts. (F) Calcified foci derived from KusaA^{NICD} cells were surrounded by a few spindle shaped cells positive for ALP (arrows). (G) Multinuclear TRAP-positive cells (arrows) appeared adjacent to the bone-like tissues derived from KusaA, implying the presence of osteoclasts. (H) No TRAP-positive cells were observed in the KusaA^{NICD}-derived tissues Scale bar—A, B: 1 mm, C, D: 250 μm, E, F: 125 μm.

such as osteoporosis by artificially modifying the Notch signaling pathway.

Acknowledgments

We thank Dr. S. Kasugai for his helpful comments on our manuscript. This work was partially supported by Grant-in-Aids for Scientific Research by the Japanese Society for the Promotion of Science (14370615, 12671763, 13771070).

References

[1] P. Bianco, M. Riminucci, S. Gronthos, P.G. Robey, Bone marrow stromal stem cells: nature, biology, and potential applications, Stem Cells 19 (2001) 180–192.
[2] A. Van Damme, T. Vanden Driessche, D. Collen, M.K. Chuah, Bone marrow stromal cells as targets for gene therapy, Curr. Gene Ther. 2 (2002) 195–209.
[3] G.A. Rodan, S. Harada, The missing bone, Cell 89 (1997) 677–680.
[4] A. Yamaguchi, T. Komori, T. Suda, Regulation of osteoblast differentiation mediated by bone morphogenetic proteins, hedgehogs, and Cbfa1, Endocr. Rev. 21 (2000) 393–411.
[5] Y.N. Jan, L.Y. Jan, HLH proteins, fly neurogenesis, and vertebrate myogenesis, Cell 75 (1993) 827–830.
[6] S. Artavanis-Tsakonas, M.D. Rand, R.J. Lake, Notch signaling: cell fate control and signal integration in development, Science 284 (1999) 770–776.
[7] F.E. Tax, J.J. Yeargers, J.H. Thomas, Sequence of C. elegans lag-2 reveals a cell-signalling domain shared with Delta and Serrate of Drosophila, Nature 368 (1994) 150–154.
[8] J.S. Mumm, E.H. Schroeter, M.T. Saxena, A. Griesemer, X. Tian, D.J. Pan, W.J. Ray, R. Kopan, A ligand-induced extracellular cleavage regulates gamma-secretase-like proteolytic activation of Notch1, Mol. Cell. 5 (2000) 197–206.
[9] S. Jarriault, C. Brou, F. Logeat, E.H. Schroeter, R. Kopan, A. Israel, Signalling downstream of activated mammalian Notch, Nature 377 (1995) 355–358.
[10] E.H. Schroeter, J.A. Kisslinger, R. Kopan, Notch-1 signalling requires ligand-induced proteolytic release of intracellular domain, Nature 393 (1998) 382–386.
[11] P.W. Sternberg, Lateral inhibition during vulval induction in Caenorhabditis elegans, Nature 335 (1988) 551–554.
[12] Y. Wakamatsu, T.M. Maynard, J.A. Weston, Fate determination of neural crest cells by NOTCH-mediated lateral inhibition and asymmetrical cell division during gangliogenesis, Development 127 (2000) 2811–2821.
[13] R. Kopan, J.S. Nye, H. Weintraub, The intracellular domain of mouse Notch: a constitutively activated repressor of myogenesis directed at the basic helix-loop-helix region of MyoD, Development 120 (1994) 2385–2396.
[14] L.A. Milner, A. Bigas, R. Kopan, C. Brashem-Stein, I.D. Bernstein, D.I. Martin, Inhibition of granulocytic differentiation by mNotch1, Proc. Natl. Acad. Sci. USA 93 (1996) 13014–13019.
[15] A. Chitnis, D. Henrique, J. Lewis, D. Ish-Horowicz, C. Kintner, Primary neurogenesis in Xenopus embryos regulated by a homologue of the Drosophila neurogenic gene Delta, Nature 375 (1995) 761–766.
[16] H. Kato, Y. Taniguchi, H. Kurooka, S. Minoguchi, T. Sakai, S. Nomura-Okazaki, K. Tamura, T. Honjo, Involvement of RBP-J in biological functions of mouse Notch1 and its derivatives, Development 124 (1997) 4133–4141.
[17] R. Kopan, E.H. Schroeter, H. Weintraub, J.S. Nye, Signal transduction by activated mNotch: importance of proteolytic processing and its regulation by the extracellular domain, Proceedings of the National Academy of Sciences of the United States of America 93 (1996) 1683–1688.
[18] E. Hirsinger, P. Malapert, J. Dubrulle, M.C. Delfini, D. Duprez, D. Henrique, D. Ish-Horowicz, O. Pourquie, Notch signalling acts in postmitotic avian myogenic cells to control MyoD activation, Development 128 (2001) 107–116.
[19] K. Penta, J.A. Varner, L. Liaw, C. Hidai, R. Schatzman, T. Quertermous, Dell induces integrin signaling and angiogenesis by ligation of alpha Vbeta3, J. Biol. Chem. 274 (1999) 11101–11109.
[20] R. Crowe, J. Zikherman, L. Niswander, Delta-1 negatively regulates the transition from prehypertrophic to hypertrophic chondrocytes during cartilage formation, Development 126 (1999) 987–998.
[21] D.J. Dallas, P.G. Genever, A.J. Patton, M.I. Millichip, N. McKie, T.M. Skerry, Localization of ADAM10 and Notch receptors in bone, Bone 25 (1999) 9–15.
[22] M. Schnabel, I. Fichtel, L. Gotzen, J. Schlegel, Differential expression of Notch genes in human osteoblastic cells, Int J. Mol. Med. 9 (2002) 229–232.
[23] A. Umezawa, T. Maruyama, K. Segawa, R.K. Shadduck, A. Waheed, J. Hata, Multipotent marrow stromal cell line is able to induce hematopoiesis *in vivo*, J. Cell. Physiol. 151 (1992) 197–205.
[24] J. Kohyama, H. Abe, T. Shimazaki, A. Koizumi, K. Nakashima, S. Gojo, T. Taga, H. Okano, J. Hata, A. Umezawa, Brain from bone: efficient "meta-differentiation" of marrow stroma-derived mature osteoblasts to neurons with Noggin or a demethylating agent, Differentiation 68 (2001) 235–244.
[25] K. Ochi, G. Chen, T. Ushida, S. Gojo, K. Segawa, H. Tai, K. Ueno, H. Ohkawa, T. Mori, A. Yamaguchi, Y. Toyama, J. Hata, A. Umezawa, Use of isolated mature osteoblasts in abundance acts as desired-shaped bone regeneration in combination with a modified poly-DL-lactic-co-glycolic acid (PLGA)-collagen sponge, J. Cell. Physiol. 194 (2003) 45–53.
[26] K. Sakamoto, O. Ohara, M. Takagi, S. Takeda, K. Katsube, Intracellular cell-autonomous association of Notch and its ligands: a novel mechanism of Notch signal modification, Dev. Biol. 241 (2002) 313–326.
[27] H. Mukohyama, M. Ransjo, H. Taniguchi, T. Ohyama, U.H. Lerner, The inhibitory effects of vasoactive intestinal peptide and pituitary adenylate cyclase-activating polypeptide on osteoclast formation are associated with upregulation of osteoprotegerin and downregulation of RANKL and RANK, Biochem. Biophys. Res. Commun. 271 (2000) 158–163.
[28] M. Fujiwara, S. Tagashira, H. Harada, S. Ogawa, T. Katsumata, M. Nakatsuka, T. Komori, H. Takada, Isolation and characterization of the distal promoter region of mouse Cbfa1, Biochim. Biophys. Acta. 1446 (1999) 265–272.
[29] B. Kern, J. Shen, M. Starbuck, G. Karsenty, Cbfa1 contributes to the osteoblast-specific expression of type I collagen genes, J. Biol. Chem. 276 (2001) 7101–7107.
[30] P. Ducy, G. Karsenty, Two distinct osteoblast-specific cis-acting elements control expression of a mouse osteocalcin gene, Mol. Cell Biol. 15 (1995) 1858–1869.
[31] P. Ducy, R. Zhang, V. Geoffroy, A.L. Ridall, G. Karsenty, Osf2/Cbfa1: a transcriptional activator of osteoblast differentiation, Cell 89 (1997) 747–754.
[32] G.S. Stein, J.B. Lian, T.A. Owen, Relationship of cell growth to the regulation of tissue-specific gene expression during osteoblast differentiation, Faseb J. 4 (1990) 3111–3123.
[33] H. Siggelkow, K. Rebenstorff, W. Kurre, C. Niedhart, I. Engel, H. Schulz, M.J. Atkinson, M. Hufner, Development of the osteoblast phenotype in primary human osteoblasts in culture: comparison with rat calvarial cells in osteoblast differentiation, J. Cell. Biochem. 75 (1999) 22–35.

[34] S.B. Doty, B.H. Schofield, Enzyme histochemistry of bone and cartilage cells, Prog. Histochem. Cytochem. 8 (1976) 1–38.
[35] G.R. Beck Jr., E.C. Sullivan, E. Moran, B. Zerler, Relationship between alkaline phosphatase levels, osteopontin expression, and mineralization in differentiating MC3T3-E1 osteoblasts, J. Cell. Biochem. 68 (1998) 269–280.
[36] S. Hitoshi, T. Alexson, V. Tropepe, D. Donoviel, A.J. Elia, J.S. Nye, R.A. Conlon, T.W. Mak, A. Bernstein, D. van der Kooy, Notch pathway molecules are essential for the maintenance, but not the generation, of mammalian neural stem cells, Genes Dev. 16 (2002) 846–858.
[37] B. Varnum-Finney, L. Xu, C. Brashem-Stein, C. Nourigat, D. Flowers, S. Bakkour, W.S. Pear, I.D. Bernstein, Pluripotent, cytokine-dependent, hematopoietic stem cells are immortalized by constitutive Notch1 signaling, Nat. Med. 6 (2000) 1278–1281.
[38] K.W. McLarren, R. Lo, D. Grbavec, K. Thirunavukkarasu, G. Karsenty, S. Stifani, The mammalian basic helix loop helix protein HES-1 binds to and modulates the transactivating function of the runt-related factor Cbfa1, J. Biol. Chem. 275 (2000) 530–538.
[39] K. Tezuka, M. Yasuda, N. Watanabe, N. Morimura, K. Kuroda, S. Miyatani, N. Hozumi, Stimulation of osteoblastic cell differentiation by Notch, J. Bone Miner. Res. 17 (2002) 231–239.
[40] M. Kurokawa, T. Tanaka, K. Tanaka, N. Hirano, S. Ogawa, K. Mitani, Y. Yazaki, H. Hirai, A conserved cysteine residue in the runt homology domain of AML1 is required for the DNA binding ability and the transforming activity on fibroblasts, J. Biol. Chem. 271 (1996) 16870–16876.
[41] D. Nofziger, A. Miyamoto, K.M. Lyons, G. Weinmaster, Notch signaling imposes two distinct blocks in the differentiation of C2C12 myoblasts, Development 126 (1999) 1689–1702.
[42] N. Takahashi, N. Udagawa, T. Suda, A new member of tumor necrosis factor ligand family, ODF/OPGL/TRANCE/RANKL, regulates osteoclast differentiation and function, Biochem. Biophys. Res. Commun. 256 (1999) 449–455.
[43] S.D. Neale, R. Smith, J.A. Wass, N.A. Athanasou, Osteoclast differentiation from circulating mononuclear precursors in Paget's disease is hypersensitive to 1,25-dihydroxyvitamin D(3) and RANKL, Bone 27 (2000) 409–416.
[44] D.E. Myers, F.M. Collier, C. Minkin, H. Wang, W.R. Holloway, M. Malakellis, G.C. Nicholson, Expression of functional RANK on mature rat and human osteoclasts, FEBS Lett. 463 (1999) 295–300.
[45] R. Kitazawa, S. Kitazawa, S. Maeda, Promoter structure of mouse RANKL/TRANCE/OPGL/ODF gene, Biochim. Biophys. Acta. 1445 (1999) 134–141.
[46] C.A. O'Brien, B. Kern, I. Gubrij, G. Karsenty, S.C. Manolagas, Cbfa1 does not regulate RANKL gene activity in stromal/osteoblastic cells, Bone 30 (2002) 453–462.

ELSEVIER

Molecular and Cellular Endocrinology 203 (2003) 105–116

MCE
Molecular and Cellular Endocrinology

www.elsevier.com/locate/mce

Islet cell hyperplasia in transgenic mice overexpressing EAT/mcl-1, a bcl-2 related gene

Kenichi Matsushita [a,b], Hajime Okita [a], Atsushi Suzuki [a], Kouji Shimoda [c], Mariko Fukuma [a], Taketo Yamada [a], Fumihiko Urano [a], Takahiro Honda [a], Makoto Sano [a], Shiro Iwanaga [b], Satoshi Ogawa [b], Jun-ichi Hata [a,1], Akihiro Umezawa [a,1,*]

[a] *Department of Pathology, Keio University School of Medicine, 35 Shinanomachi, Shinjuku-ku, Tokyo 160-8582, Japan*
[b] *Department of Medicine, Keio University School of Medicine, 35 Shinanomachi, Shinjuku-ku, Tokyo 160-8582, Japan*
[c] *Laboratory Animal Center, Keio University School of Medicine, 35 Shinanomachi, Shinjuku-ku, Tokyo 160-8582, Japan*

Received 1 July 2002; accepted 28 January 2003

Abstract

EAT/mcl-1 (EAT), a bcl-2 related anti-apoptotic gene, is up-regulated at the early stage of differentiation of human embryonal carcinoma cells; cells which serve as a model for early embryogenesis. We generated transgenic mice for the human EAT gene driven by the EF1α promoter in order to elucidate its functional role in vivo. Histologically, these mice exhibited hyperplasia of Langerhans islet cells; pancreatic cell regions composed of both insulin- and glucagon-producing cells. Furthermore, Bax and Bag-1—possible heterodimeric partners for EAT in the anti-apoptotic process—were up-regulated in islets isolated from the EAT transgenic mice. The insulin tolerance test exhibited no significant difference between the EAT transgenic mice and non-transgenic mice, indicating that islet cell hyperplasia was not due to insulin resistance. In conclusion, EAT transgenic mice exhibit hyperplasia of pancreatic β cells. EAT may inhibit apoptosis of β cells, allowing these cells to circumvent the process of apoptosis until the adult stage.
© 2003 Elsevier Science Ireland Ltd. All rights reserved.

Keywords: Apoptosis; EAT; Islet β-cell; mcl-1; Transgenic mice

1. Introduction

We isolated human EAT/mcl-1 (EAT), a bcl-2 related gene, as a gene up-regulated at an early stage of differentiation of an embryonal carcinoma (EC) cell line designated NCR-G3 (Umezawa et al., 1996). Human EC cell lines serve as model systems for early human embryogenesis based upon their multiple differentiation potential. NCR-G3, derived from a testicular EC, differentiates into multiple lineages, including trophectoderm cells, following exposure to retinoic acid (Hata et al., 1992). Human EAT (hEAT) was originally identified as mcl-1, a gene whose expression is induced during differentiation of myeloid leukemia cells (Kozopas et al., 1993); however, we further established that it is likewise up-regulated during early differentiation of EC cells (Umezawa et al., 1996). Recently, we also cloned a murine orthologue of hEAT (murine EAT, mEAT) (Okita et al., 1998).

The EAT gene is considered to be a member of the bcl-2 related gene family based upon its possession of the bcl-2 homology (BH) domains 1, 2, 3 and 4 (Bingle et al., 2000; Kroemer, 1997; Revilla et al., 1997). Bcl-2-related genes display either positive or negative regulatory effects on apoptosis in vitro and in vivo (Adams and Cory, 1998; Chao and Korsmeyer, 1998; Reed, 1998). Previous studies have established that Bcl-2, Bcl-xL, Bcl-w, Bfl-1 and A1 are anti-apoptotic molecules while Bax, Bak, Bcl-xS, Bad, Bid, Bik and Hrk are pro-apoptotic molecules (Boise et al., 1993; Chittenden et al., 1995; D'Sa-Eipper et al., 1996; Gibson et al., 1996; Inohara et al., 1997; Lin et al., 1996; Wang et al., 1996;

* Corresponding author. Tel.: +81-3-5363-3764; fax: +81-3-3353-3290.
E-mail address: umezawa@1985.jukuin.keio.ac.jp (A. Umezawa).
[1] Present address: The National Center for Child Health and Development Research Institute, Tokyo 154-8567, Japan.

0303-7207/03/$ - see front matter © 2003 Elsevier Science Ireland Ltd. All rights reserved.
doi:10.1016/S0303-7207(03)00095-9

Yang et al., 1995a). Recent studies revealed that EAT inhibits apoptosis in vitro and in vivo (Akgul et al., 2000a,b; Ando et al., 1998; Matsushita et al., 1999; Moulding et al., 2000; Reynolds et al., 1994; Sano et al., 2001, 2000).

The in vivo effects of Bcl-2 related genes have been investigated in transgenic or knock-out mice. Bcl-2 transgenic mice are known to promote cell survival in B cells, T cells and thymocytes (McDonnell et al., 1989; Sentman et al., 1991; Siegel et al., 1992; Strasser et al., 1991). Mice deficient for bcl-2 display increased apoptosis in selected tissues (Veis et al., 1993). These phenotypes reflect the anti-apoptotic functions established for bcl-2 in vitro. On the other hand, bax transgenic mice present with increased apoptosis in T cells and mice deficient for bax demonstrate hyperplasia of thymocytes and B cells (Brady et al., 1996a,b; Knudson et al., 1995). Male Bax-deficient mice are infertile with atrophic adult testes and an empty epididymis and vas deferens; a complete cessation of mature sperm cell production occurs in these mice (Knudson et al., 1995). These phenotypes result from the pro-apoptotic functions of Bax.

We generated three lines of EAT transgenic mice, driven by the EF1α promoter, to investigate in vivo the role of EAT during development. Our aim was to determine whether overexpression of the hEAT gene would cause anti-apoptotic effects in vivo similar to the bcl-2 gene. In this report, we show that EAT transgenic mice develop islet cell hyperplasia reflecting inhibition of apoptosis of β cells.

2. Materials and methods

2.1. Generation of transgenic mice for hEAT gene

To generate transgenic mice that express hEAT, a transgene was constructed with the human EF1α promoter linked to hEAT (EF1α–EAT) (Hanaoka et al., 1991) (Fig. 1A). The PvuI fragment of EF1α–EAT (6.7 kb) was purified and dissolved in 10 mM Tris, 0.25 mM EDTA (pH 7.4) at a concentration of 3 μg/ml. The production of transgenic mice was performed according to standard procedures (Hogan et al., 1986). In brief, a DNA solution (3 μg/ml) was microinjected into the male pronuclei of fertilized mouse eggs taken from superovulated B6C3F1 (C57BL/6 × C3H/He) females. The injected eggs were surgically transferred to the oviducts of B6C3F1 pseudopregnant female mice. Transgene-bearing mice were selected by Southern blot analysis of tail DNA (10 μg) hybridized with the EF1α–EAT probe of the 6.7-kb PvuI–PvuI fragment. Orientation of the transgene integrated into the chromosome and copy numbers of each line were analyzed by Southern blot hybridization. Copy numbers were calculated by the

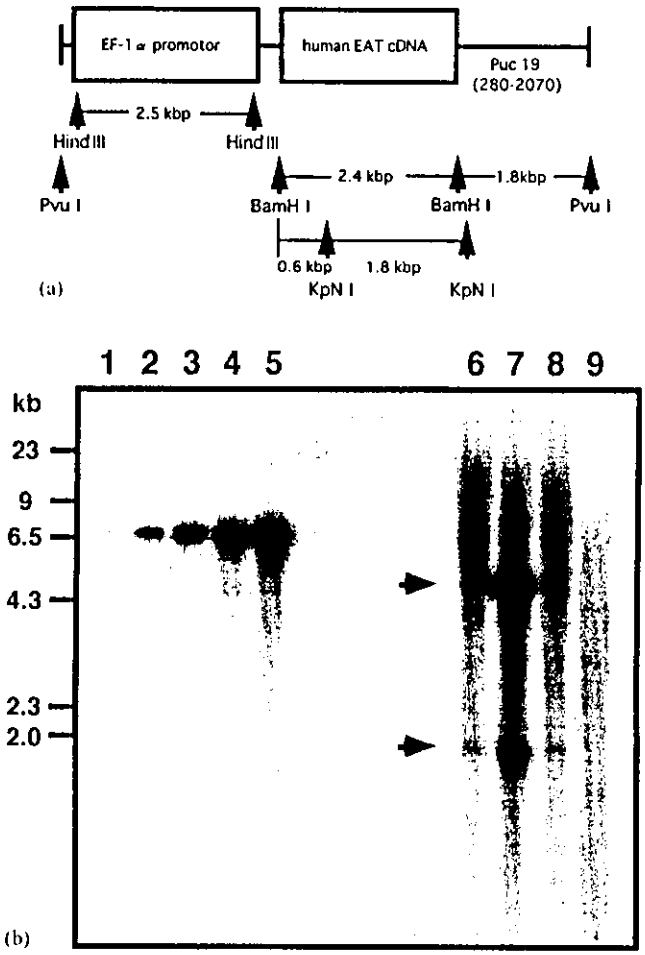

Fig. 1. Generation of EAT transgenic mice. (A) Schema of the EF1α-hEAT (EF1α-EAT) transgene construct. The PvuI fragment was used as the transgene. The same 6.7 kb PvuI fragment was used as a probe for Southern blot hybridization. This hEAT transgene, driven by the EF1α promoter, was injected into the fertilized eggs. (B) Southern blot analysis of tail DNA from heterozygote transgenic lines. The copy numbers of the transgene per diploid genome for each line are: 20 (E2), 150 (E3), and 20 (E12), as shown in lane 6–8, respectively. KpnI-digested tail genomic DNA was hybridized with a ^{32}P-labeled EF1α-EAT probe. Kilobase size markers are shown on the left. Arrows indicate the bands of EF1α-EAT DNA fragments digested with KpnI. Orientation of the hEAT transgene was determined to be head-to-tail in all lines. Lanes 1–5 represent controls for transgene fragment copy numbers (lane 1: 1 copy, lane 2: 10 copies, lane 3: 20 copies, lane 4: 50 copies, lane 5: 100 copies). Lane 9 represents a non-transgenic control.

bio-imaging analyzer (BAS2000, Fuji Film, Japan), using the transgene fragment mixed with mouse genomic DNA as copy number controls. The founder mice obtained were assigned with a number preceded with a letter E, like E2 or E3. Offsprings were screened by detecting the 1097-bp hEAT fragment in the tail DNA with polymerase chain reaction (PCR) using a set of appropriate primers. The sequences of the primers used were as follows; the sense primer: 5′ CTGCATCGAACCATTAGCAG 3′, and the antisense primer: 5′ TACAACCAGTCTGCATACAG 3′.

Animals were housed in micro-isolation cages on wood shavings and observed daily for evidence of weakness. The study was approved by the Keio University School of Medicine Care of Experimental Animals Committee.

2.2. Expression of the hEAT transgene compared to endogenous mEAT

Langerhans islets were isolated by collagenase digestion method (Gotoh et al., 1985; Lacy and Kostianovsky, 1967). RNA extraction from islets and other tissues were performed using ISOGEN (Wako, Osaka, Japan), following the manufacturer's instructions. First strand cDNA synthesis was performed using First-Strand cDNA Synthesis Kit (Pharmacia Biotech, Uppsala, Sweden). The PCR reaction was carried out using the synthesized cDNA in a reaction with 50 pmol of each primer and 2.5 Units of Taq DNA polymerase (Toyobo, Osaka, Japan) in a buffer containing 10 mM Tris–HCl (pH 8.3), 50 mM KCl, 2.5 mM $MgCl_2$, 0.1% TritonX-100, and each deoxyribonucleoside triphosphate at 100 μM. The reaction mixtures were then amplified through 35 cycles at 95 °C for 2 min, 48 °C for 1 min, and 72 °C for 1 min, followed by a final extension cycle at 72 °C for 5 min. The primer pairs which detected both hEAT transgene and endogenous mEAT separately are; sense: 5′ CATCGAACCATTAGCAG 3′, and antisense: 5′ GAGCACTTTTCCCATGTATT 3′.

β-actin cDNA was amplified as a control for RNA integrity. The primers used for the β-actin reaction to amplify a 729-kb fragment were; sense: 5′ GTCCCTGTATGCCTCTGGTCGTAC 3′, and antisense: 5′ GCAGCTCAGTAACAGTCCGCCTAG 3′. The PCR amplifications were carried out in an automated thermal cycler (Minicycler, MJ Research, Inc., MA, USA). After electrophoresis of PCR products, the gel was stained with vistra green (Amersham, Buckinghamshire, England) and the DNA bands were visualized using the Fluor Imager (Molecular Dynamics Inc., CA, USA).

2.3. Comparison of the expression level for hEAT in islets of all three lines

Langerhans islets of all three transgenic lines were isolated and RNA extraction from islets was performed. After synthesizing first strand cDNA, the PCR reaction was carried out using the synthesized cDNA through 20 cycles (at 94 °C for 2 min, at 50 °C for 2 min, at 72 °C for 2 min) using an automated thermal cycler (Minicycler, MJ Research, Inc.). The primer pair which specifically detects hEAT but does not detect endogenous mEAT is; sense: 5′ ATTGATTACCCGCCGAA 3′, and antisense: 5′ GGTCAAATGGAAGGAAC 3′.

β-actin cDNA was amplified as a control for RNA integrity. After electrophoresis of PCR products, the gel was stained with vistra green (Amersham) and the DNA bands were visualized using the Fluor Imager (Molecular Dynamics Inc.).

2.4. Differential hybridization of Atlas™ Mouse cDNA expression arrays

Transgenic islets were isolated from a 8-month-old mouse of the E2 line and non-transgenic islets were isolated from a 3-month-old non-transgenic mouse. RNA extraction was performed using ISOGEN (Wako). Universal Ribo Clone cDNA synthesis system (Promega, WI) was used for the first and second cDNA strand synthesis. RNA suspended in 9.4 μl nuclease-free water was mixed with 1 μl CDS primer (0.02 μM; Clontech, Palo Alto, CA). RNA and the primer mix were incubated at 70 °C for 5 min, then at 50 °C for 2 min. Four microliter of 5 × First Strand buffer, 1 μl of RNasin Ribonuclease Inhibitor (40 Units/μl), 2.5 μl of Sodium Pyrophosphate (40 mM) and 1.5 μl of AMV Reverse Transcriptase (20 Units/μl) were added to the reaction mixture on ice and incubated at 42 °C for 4 h. The dsDNA was treated to synthesize blunt ends and 0.4 μl of T4 DNA Polymerase was added followed by incubation at 37 °C for 10 min. The free primer was removed by MicroSpin S-400 column (Amersham Pharmacia Biotech, Sweden).

Blunt ended cDNAs were ligated, for 15 h at 15 °C, to a specially designed linker-primer, 'LL-RI' (Ko et al., 1990a):

LL-RIA: 5′ GAGATATTAGAATTCTACTC-3′
LL-RIB: 3′-TATAATCTTAAGATGAGp-5′

Since the protruding end is not adhesive, a single molecule of the linker was attached to each end of the cDNA in an orientation-specific manner (thus called 'lone linker') (Ko et al., 1990a). Amplification of the cDNA fragments was then performed by PCR through 20 cycles (at 94 °C for 2 min, at 50 °C for 2 min, at 72 °C for 2 min) using an automated thermal cycler (Minicycler, MJ Research, Inc.). Free primer was removed by MicroSpin S-400 column (Amersham). Amplified cDNA was labeled with 50 μCi [α-^{32}P] dCTP (3000 Ci/μmole) using a random primer labeling kit (Amersham). The free ^{32}P was removed by Sephadex G-50 column (Amersham).

Equal amounts of labeled cDNA (1×10^8 cpm) from transgenic and non-transgenic islets were then hybridized to two Atlas™ Mouse cDNA expression arrays in 5 ml of hybridization solution for 18 h at 65 °C. The expression arrays were washed in solution 1 (2 × SSC and 1% SDS) for 60 min at room temperature. A second wash was performed at 65 °C for 40 min in solution 2

(0.1 × SSC and 0.5% SDS). The filters were then exposed on Imaging plates (Fuji Film) for 48 h and analyzed by BAS 2000 (Fuji Film).

2.5. Histology

For routine histology, pancreatic tissue was fixed in 10% formalin and embedded in paraffin. Sections (6 μm) were processed and stained with hematoxylin and eosin. All cases that demonstrated islet cell hyperplasia and several cases with normal islets were then serially sectioned for immunohistochemistry. Immunohistochemical staining was performed with a guinea pig anti-insulin antibody (DakoCytomation Co. Ltd., Copenhagen, Denmark) and a rabbit anti-glucagon antibody (Dako).

2.6. Quantitative area measurement of islets

For quantitative area measurement of islets, we used the MAC SCOPE (Mitani, Inc., Chiba, Japan) software program for analysis. For analysis, 1 randomly sectioned slide from each paraffin block, representing a single animal, was used. The area to be measured by the MAC SCOPE (1–3 mm^2) was chosen to include the maximal islet detected on the slide. From this chosen area, the ratio of the islet cell to the pancreatic area was measured.

2.7. Measurement of glucose and insulin

Mice were fasted overnight and glucose was administered intraperitoneally at 2 mg glucose/g body weight (BW). Fifteen minutes after glucose administration, blood was collected from the right cardiac ventricle to measure blood glucose and serum insulin levels. Blood glucose was measured immediately using whole blood by the Advantage (Yamanouchi Co., Ltd, Tokyo, Japan) kit. Serum insulin levels were measured by EIA using the ELSIA-F-Insulin (International Reagents Corporation, Kobe, Japan) kit and human insulin standards.

In the insulin tolerance test, human insulin (0.5 Units/kg) was injected intraperitoneally in anesthetized adult mice (5–8 months) after fasting overnight. Blood samples were taken from the tail vein.

All assays were performed in duplicate.

2.8. Statistical analyses

Descriptive statistics, ANOVA followed by Bonferroni/Dunn test and regression analysis, were performed. A P value less than 0.05 denoted the presence of a statistically significant difference.

3. Results

3.1. Generation of EAT transgenic mice

We generated several lines of EAT transgenic mice. The EAT gene was driven by the EF1α promoter (Fig. 1A). Initial screening was carried out by Southern blot analysis of tail DNA using an EF1α–EAT probe; mice incorporating the integrated gene were determined by positive hybridization signals (Fig. 1B). The transgene is observed to be intact in each line and is integrated in a head-to-tail fashion in all lines. The copy number, as determined by phosphoimaging, was 20 for the E2 line, 150 for the E3 line and 20 for the E12 line. All three founder animals were subsequently bred with F1 (C57BL/6 and C3H/He) animals and offsprings heterozygous for the transgene were screened by PCR.

3.2. Analysis of hEAT expression

Offsprings from the three original founders—designated E2, E3, and E12—were found to express the hEAT transgene ubiquitously in tissues including the liver, kidney, heart, lung, pituitary gland, and Langerhans islets by RT-PCR, although expression levels varied among tissues. Comparison of hEAT transgene expression with endogenous mEAT expression showed that Langerhans islets exhibited higher expression levels of hEAT transgene compared to other tissues (Fig. 2A).

We next analyzed hEAT expression in Langerhans islets of all three transgenic lines by RT-PCR. As shown in Fig. 2B and C, the expression level in the E2 line was much higher than in the other two lines. The expression level (hEAT/β-actin) was lowest in the E3 line; however, the difference between the E3 and E12 lines was subtle.

The expression of the transgene was found to be below levels detectable by Northern blot analysis. This is not due to the construct of the transgene as the same transgene is expressed at high levels in cultured fibroblast clones as determined by RNA blot analysis (Sano et al., 2001). Nevertheless, transgenic mice which express EAT at high levels may possibly be lethal during embryogenesis.

3.3. Enlargement of islets in EAT transgenic mice

Histological examination revealed enlargement of pancreatic Langerhans islets of EAT transgenic mice compared with non-transgenic mice (Fig. 3A–C). To determine the functional composition of these enlarged lesions, we performed immunohistochemical analysis with antibodies to insulin and glucagon. The majority of the cells were positive for insulin while cells positive for glucagon were observed only sporadically (Fig. 3D and E). The same immunohistochemical pattern was observed in all the three transgenic lines produced. The

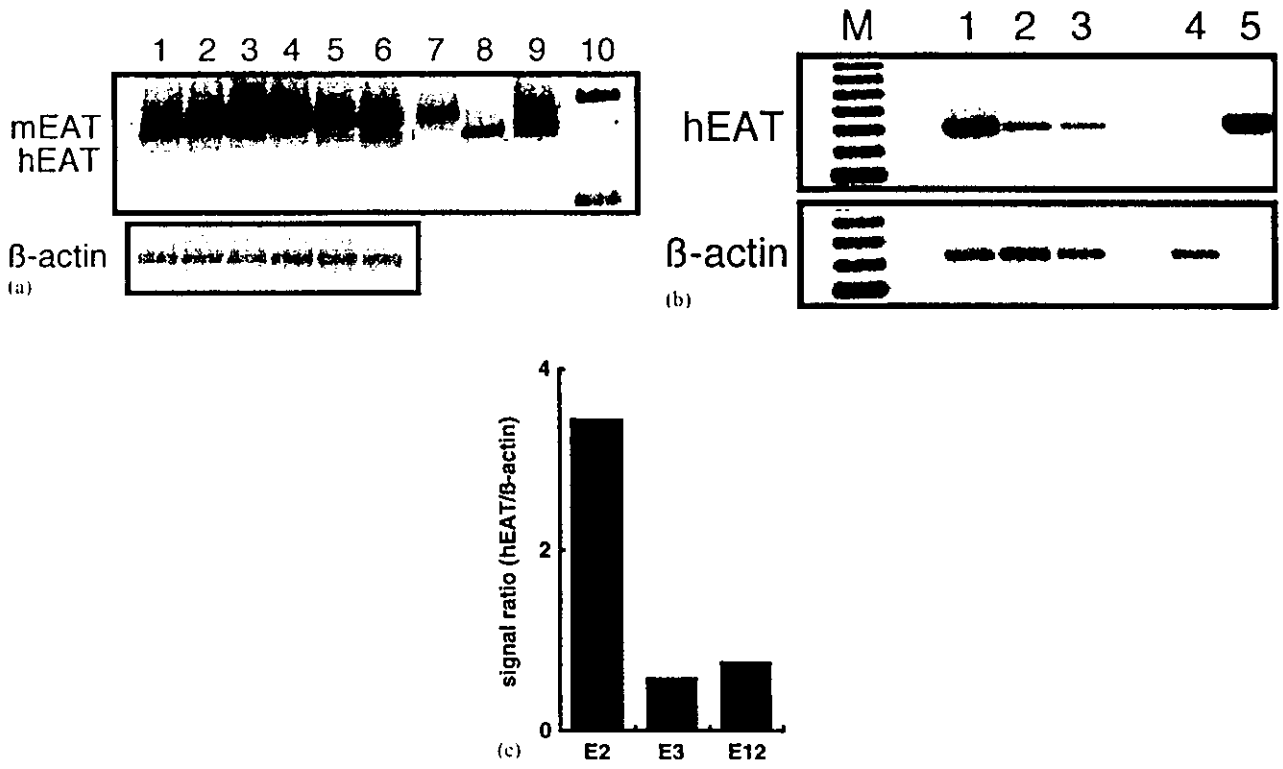

Fig. 2. Expression of the hEAT transgene by RT-PCR. Islet cells were isolated by collagenase treatment. (A) Expression of the hEAT transgene as assayed in various tissues compared with endogenous mEAT by RT-PCR. RT-PCR was performed with a primer set which detected both the hEAT transgene and endogenous mEAT but displayed two different bands (lane 1: liver; lane 2: kidney; lane 3: heart; lane 4: lung; lane 5: pituitary gland; lane 6: isolated islet cells from a E2 transgenic mouse). Controls included lane 7: liver from non-transgenic mouse (as a positive control for mEAT); lane 8: NCR-G3 cells, a human EC cell line (as a positive control for hEAT); and lane 9: a plasmid DNA mixture containing equal amounts of mouse and hEAT (as a quantitative control of the primer set). A 100 bp ladder is shown as a size marker in lane 10 (upper band: 400 bp; lower band: 300 bp). β-Actin (729 bp) RT-PCR products are shown to demonstrate the integrity of the isolated RNA (lower column). Langerhans islets (lane 6) exhibited higher expression levels of hEAT compared to other tissues. (B) Expression of the hEAT transgene in isolated islets from all three transgenic lines. RT-PCR was performed with a primer set which detected only the hEAT gene without detecting the endogenous mEAT gene (lane 1: E2; lane 2: E3; lane 3: E12; lane 4: non-transgenic mouse; lane 5: NCR-G3 cells). Islets from a non-transgenic mouse and NCR-G3 cells served as negative and positive controls, respectively. A 100 bp ladder is shown as a size marker in lane M. β-Actin (729 bp) RT-PCR products are shown to demonstrate the integrity of the isolated RNA (lower column). The β-actin band was not detected in human NCR-G3 cells (lane 5), since the primers were prepared specifically for the murine β-actin gene, and not for the human gene. (C) Bar graph representing the signal intensity ratio of hEAT to β-actin (hEAT/β-actin) for (B). A difference in hEAT expression can be detected in the three lines. The E2 line showed a higher expression level compared with the other two lines. The expression level in the E3 line was lowest; however, the difference between the E3 and E12 lines was subtle.

enlargement of islets was considered to be hyperplasia rather than adenoma. These hyperplastic islets in EAT transgenic mice develop between 4 and 24 months of age and were macroscopically visible in older animals.

For quantitative area measurements of the islet cell area, three lines of transgenic mice were used: E2, E3, and E12. Of the 29 transgenic mice studied, 7 were from the E12 line (ages ranging from 5 to 16 months), 10 were from the E2 line (ages ranging from 4 to 17.5 months), and 12 were from the E3 line (ages ranging from 7 to 14 months). Fourteen non-transgenic mice were studied (ages ranging from 4.5 to 14 months). Quantitative area measurement revealed the ratio of islet cell area to total pancreatic area in E2 or E12 transgenic mice to be higher than that in non-transgenic mice (Fig. 4). The ratio of islet cell area to total pancreatic area in E12 transgenic mice was significantly higher than that in non-transgenic mice ($P = 0.0021$). In contrast, the E3 transgenic mice did not show any increase in the islet cell area as compared to the non-transgenic mice.

3.4. Detection of other bcl-2 related genes in transgenic islet cells

We used the differential hybridization technique of Atlas™ Mouse cDNA expression array to identify genes which are differentially expressed either in EAT transgenic or non-transgenic islet cells. As shown in Fig. 5, Bax and Bag-1 were up-regulated in EAT transgenic islet cells compared with non-transgenic islet cells. Expression was not noted for Bcl-2, Bcl-xL, Bad, Bak, Bcl-w and Bid in either transgenic or non-transgenic islets. Selenoprotein, a glutathione peroxidase, and β-actin were used as internal controls and were expressed

(A)

(B)

(C)

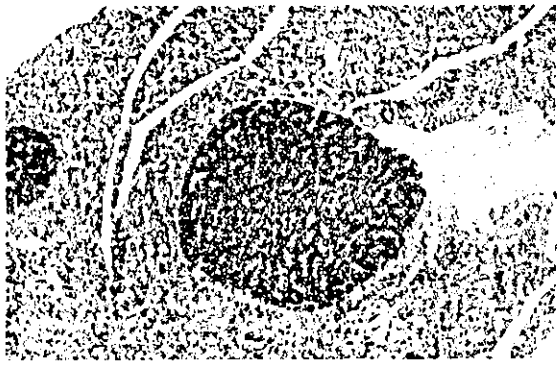

(D)

(E)

Fig. 3

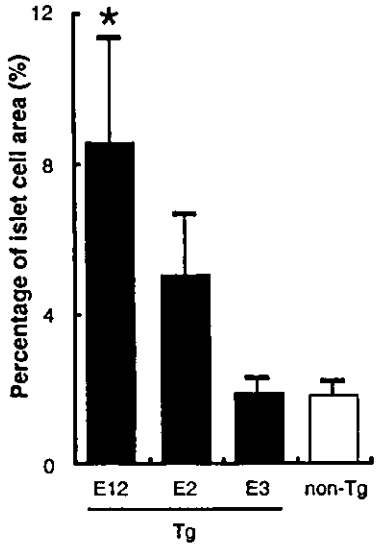

Fig. 4. Percentage of islet cell area to pancreas area. Three lines of transgenic mice were used: E2, E3, and E12. Of the 29 transgenic mice studied, 7 were from the E12 line (ages ranging from 5 to 16 months), 10 were from the E2 line (ages ranging from 4 to 17.5 months), and 12 were from the E3 line (ages ranging from 7 to 14 months). Fourteen non-transgenic mice were studied (ages ranging from 4.5 to 14 months). Each area was calculated from the H&E stained photos. Error bars represent SEM. Tg, transgenic mice; non-Tg, non-transgenic mice. $^{*}P < 0.05$ vs non-Tg.

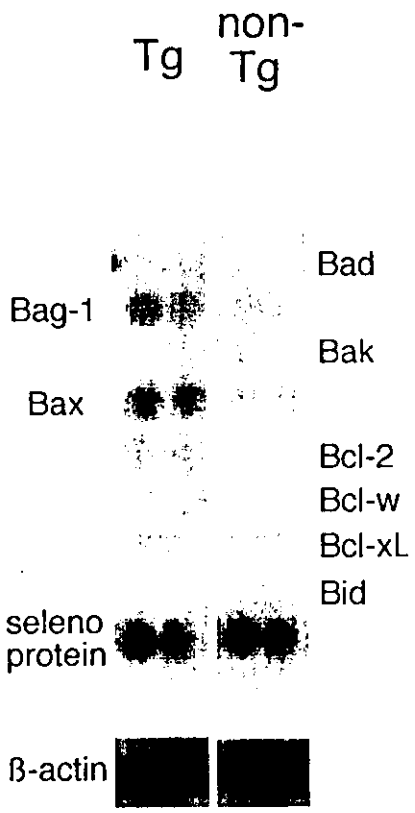

Fig. 5. Differential hybridization of cDNA expression arrays of isolated islets. The expression of bcl-2 related genes in transgenic islets was compared to expression in non-transgenic islets. The left and right panels represent expression array membranes hybridized with cDNA from transgenic and non-transgenic islets, respectively. Bax and Bag-1 were up-regulated in EAT transgenic islets compared with non-transgenic islets. Expression was not noted for Bcl-2, Bcl-xL, Bad, Bak, Bcl-w and Bid in either transgenic or non-transgenic islets. Selenoprotein, a glutathione peroxidase, and β-actin were used as internal controls and were expressed at similar levels in both EAT transgenic and non-transgenic mouse. Tg, transgenic mice; non-Tg, non-transgenic mice.

at similar levels in both EAT transgenic and non-transgenic mouse. These findings suggest that EAT participates in the control of apoptosis in islet cells.

3.5. *Insulin secretion in the hyperplastic islets*

We next measured serum insulin levels by ELISA to test the insulin secretion ability of these hyperplastic islets. Serum insulin levels were measured 15 min after intraperitoneal glucose administration following overnight fasting. As shown in Fig. 6A, a trend towards higher serum insulin levels was observed in the EAT transgenic mice; however, this difference was not statistically significant.

Fatty metamorphosis of the liver was observed in EAT transgenic mice which exhibited exceedingly high levels of serum insulin (Fig. 7). A trend towards lower blood glucose levels was observed in the transgenic mice which produced these high serum insulin levels; however, this difference was not as marked as the difference in serum insulin levels between transgenic and non-transgenic animals (data not shown).

We also assessed insulin sensitivity by an i.p. insulin tolerance test. The insulin tolerance test on E12 mice showed no significant difference in the hypoglycemic response to insulin between transgenic and non-transgenic mice (Fig. 6B). We therefore concluded that the changes we observed in islet size were not due to insulin resistance.

Fig. 3. Islet cell hyperplasia in transgenic mice overexpressing EAT. (A) Macroscopic findings of islet cell hyperplasia in an EAT transgenic mouse. Many large tumors were observed in the pancreas (as indicated by arrowheads). This photo shows the pancreas from a 8-month-old mouse from the E2 line. (B) Hyperplasia of the islets of Langerhans in the EAT transgenic mice. This specimen was prepared from a 16-month-old mouse from the E12 line. H&E staining. Original magnifications, × 20. (C) Normal appearance of islets in a 12-month-old non-transgenic mouse from the E12 line. H&E staining. Original magnifications, × 20. (D–E) Immunohistochemical analysis for insulin (D) and glucagon (E). Specimens were prepared from a 16-month-old EAT transgenic mouse from the E12 line. The majority of the enlarged Langerhans islets were positive for insulin while cells positive for glucagon were observed only sporadically. Thus, the enlargement of islets was considered to be hyperplasia. Original magnifications, × 40.